



Single-cell RNA-sequencing provides new insights into the cell-specific expression patterns and transcriptional regulation of photosynthetic genes in bermudagrass leaf blades

Bing Zhang ^{a,*}, Ziyuan Ma ^a, Hailin Guo ^b, Si Chen ^a, Jianxiu Liu ^b

^a College of Animal Science and Technology, Yangzhou University, Yangzhou 225009, China

^b Institute of Botany, Jiangsu Province and Chinese Academy of Sciences, Nanjing 210014, China



ARTICLE INFO

Keywords:

Bermudagrass
Single-cell RNA-Sequencing
Photosynthesis
Malic enzyme
Starch
Transcription factor

ABSTRACT

As an important warm-season turfgrass species, bermudagrass (*Cynodon dactylon* L.) flourishes in warm areas around the world due to the existence of the C4 photosynthetic pathway. However, how C4 photosynthesis operates in bermudagrass leaves is still poorly understood. In this study, we performed single-cell RNA-sequencing on 5296 cells from bermudagrass leaf blades. Eight cell clusters corresponding to mesophyll, bundle sheath, epidermis and vascular bundle cells were successfully identified using known cell marker genes. Expression profiling indicated that genes encoding NADP-dependent malic enzymes (NADP-MEs) were highly expressed in bundle sheath cells, whereas NAD-ME genes were weakly expressed in all cell types, suggesting C4 photosynthesis of bermudagrass leaf blades might be NADP-ME type rather than NAD-ME type. The results also indicated that starch synthesis-related genes showed preferential expression in bundle sheath cells, whereas starch degradation-related genes were highly expressed in mesophyll cells, which agrees with the observed accumulation of starch-filled chloroplasts in bundle sheath cells. Gene co-expression analysis further revealed that different families of transcription factors were co-expressed with multiple C4 photosynthesis-related genes, suggesting a complex transcription regulatory network of C4 photosynthesis might exist in bermudagrass leaf blades. These findings collectively provided new insights into the cell-specific expression patterns and transcriptional regulation of photosynthetic genes in bermudagrass.

1. Introduction

Plant leaves are heterogeneous organs consisting of epidermis cells, mesophyll cells, vascular cells and other cell types with different functions (Khoshravesh et al., 2022). Through harvesting photons in photosystems, leaf mesophyll cells could efficiently convert solar energy into electrochemical energy to drive CO₂ fixation and carbohydrate synthesis in the Calvin-Benson cycle. Leaf epidermis cells protect mesophyll cells from dehydration, whereas vascular cells are mainly responsible for substance transmission and exchange. Different plant species have evolved diverse leaf shapes and cell compositions to maximize the efficiency of photosynthesis in their living environments (Fernández-Marín et al., 2020). Understanding the anatomical and physiological adaptation mechanisms of plant species with high photosynthesis efficacy could provide essential clues to breed superior grain crops for the ever-growing global population (Ermakova et al.,

2020).

In recent years, the development and application of single-cell RNA-sequencing (scRNA-seq) technology has refined leaf gene expression profiles of many plant species to the single-cell level (Liu et al., 2022). For example, a single-cell transcriptomic atlas of developing *Arabidopsis* leaves successfully identified 14 cell populations and characterized metabolic differences among different cell types (Tenorio Berriño et al., 2022). Four studies further revealed distinct features of the different vascular, mesophyll and stomata cell types in *Arabidopsis* leaves (Kim et al., 2021; Liu et al., 2020; Lopez-Anido et al., 2021; Procko et al., 2022). A single-cell transcriptome atlas of rice seedlings identified 15 leaf cell populations and revealed that common transcriptome features were shared between leaves and roots in the same tissue layer, whereas another study successfully used PEG-mediated protoplast transfection and scRNA-seq to identify 35 possible targets of rice transcription factor (TF) OsNAC78 (Wang et al., 2021; Xie et al., 2020). ScRNA-seq of maize

* Corresponding author.

E-mail address: bingzhang@yzu.edu.cn (B. Zhang).

leaves not only revealed that maize bundle sheath cells were differentiated into abaxial and adaxial types with different functions but also unveiled many key transcription factors regulating maize mesophyll cell development (Bezrutczyk et al., 2021; Tao et al., 2022). Additionally, scRNA-seq were also used to dissect the metabolism of catechin esters in tea leaves, the cell differentiation and development in peanut leaves, the early response to *Botrytis cinerea* infection in woodland strawberry leaves, as well as adaxial and abaxial mesophyll differentiation in *Brassica rapa* (Bai et al., 2022; Guo et al., 2022; Liu et al., 2021; Wang et al., 2022). The results of these studies greatly expanded our understanding of the structure, function and development of plant leaves.

Bermudagrass (*Cynodon dactylon* L.) is an important warm-season turfgrass species and is widely used to produce beautiful and uniform turf for home lawns, public parks, golf courses, and sport fields in warm regions around the world (Xu et al., 2022). As a member of the PACMAD (acronym for Panicoideae, Aristidoideae, Chloridoideae, Micrairoideae, Arundinoideae, and Danthonioideae) clade of grasses, bermudagrass has high photosynthesis efficiency due to the existence of the C4 photosynthetic pathway (Chen et al., 1969; Zhang et al., 2018). Half a century ago, Hatch and Kagawa observed that the activity ratio of NAD-dependent malic enzyme (NAD-ME) to NADP-dependent malic enzyme (NADP-ME) in leaf extracts of *C. dactylon* plants is four-fold, suggesting bermudagrass might belong to the NAD-ME type of C4 grass (Hatch and Kagawa, 1974). However, whether other types of C4 photosynthetic pathway exist in bermudagrass is elusive because the genes and enzymes participating in photosynthesis remain uncharacterized.

In this study, we analyzed the gene expression profiles of different cell types in bermudagrass leaf blades using scRNA-seq. The results indicated that NADP-ME genes were highly expressed in bundle sheath cells, whereas NAD-ME genes were weakly expressed in all cell types. Additionally, starch synthesis and degradation-related genes were also found to be preferentially expressed in different cell types. Gene co-expression analysis further revealed that multiple TFs might be involved in the expression regulation of different C4 photosynthesis-related genes. These results not only provided new insights into the cell-specific expression patterns and transcriptional regulation of photosynthetic genes in bermudagrass but also testified the usage of scRNA-seq technology in photosynthesis research.

2. Materials and methods

2.1. Plant material and growth conditions

C. dactylon cultivar Yangjiang with an assembled reference genome sequence was used in this study (Zhang et al., 2022). The bermudagrass turf were grown in turfgrass plots of Yangzhou University (longitude and latitude: 32°35'N, 119°40'E; soil type: 80% river sand and 20% peat soil) under routine management conditions (irrigation: keep the soil moist as required; fertilization: four times/year with compound fertilizer at a concentration of 5 g/m²; mowing: one time/month). Healthy bermudagrass plants at fast growing stage (about 5 cm in height, six expanded leaves in shoots) were randomly collected at 3 p.m. from May 10, 2022 to May 12, 2022 (season: early summer, weather: sunny, day average temperature: 25–27 °C).

2.2. Microscopy

The middle sections of leaf blades at the 2nd leaf position (The fully expanded leaves of bermudagrass plants were numbered orderly from top to bottom as 1st leaf position, 2nd leaf position, 3rd leaf position, etc. Among which the 2nd leaf position was the easiest to collect fresh and homogeneous samples) were harvested and immersed in FAA fixation buffer for 24 h. After dehydration in an ethanol series (60, 70, 85 and 95%), the leaf blades were embedded in paraffin. Transverse sections

(15 µm thick) were cut with a Leica VT 1000 S vibratome (Leica, Nussloch, Germany) and mounted on glass slides. The slides were stained with Safranin O-Fast Green solution (1% Safranin O and 0.5% Fast Green), 0.1% Phloroglucinol and I₂-KI solution (1% KI and 0.3% I₂) for cell wall/cytoplasm, lignin and starch, respectively. The sections were observed and photographed using a Jiangnan BM2000 light microscope (Jiangnan Optics, Nanjing, China).

2.3. Leaf protoplast isolation

Protoplasts were isolated from the middle sections of leaf blades at the 2nd leaf position using an enzymatic digestion method specially optimized for bermudagrass (Chen et al., 2023). Briefly, 2 g of leaf blade sections were firstly teared into long strips with a length of 0.5 mm using sharp-pointed forceps. The obtained leaf strips were immediately immerged in 30 ml of enzyme solution containing 0.6 M of mannitol, 4% (w/v) cellulase 'Onozuka' R10 (Yakult Pharmaceutical, Tokyo, Japan) and 0.8% (w/v) macerozyme R10 (Yakult Pharmaceutical), 20 mM KCl, 10 mM CaCl₂, 20 mM MES-KOH (pH 5.7) and 0.1% BSA. The moist leaf strips were vacuumed (about 0.1 MPa) for 10 min in darkness at 26 °C to promote the infiltration of enzyme solution. The enzymatic digestion reactions were then carried out in a horizontal shaker at 40 rpm, 26 °C in darkness for 2 h. The status of leaf strips was observed in a 30-min interval to check the digestion efficiency. The obtained protoplasts were filtered through a 50 µm cell strainer (Sigma-Aldrich, Shanghai, China), resuspended with 10 ml of suspension solution containing 154 mM NaCl, 125 mM CaCl₂, 5 mM KCl and 2 mM MES-KOH (pH 5.7), washed three times with 8% mannitol buffer, and counted using a hemocytometer. The activities of protoplasts were determined by fluorescein diacetate staining, and protoplasts with >90% activity were selected for following bulk RNA-seq and scRNA-seq analyses.

2.4. RT-qPCR

To check the gene expression variation during the protoplast preparation process, total RNA was extracted from the isolated protoplast cells using RNApure Plant kit (Tiangen, Beijing, China) at different time-points after enzymatic digestion (leaf blade total RNA was used to represent the zero time-point). cDNA was synthesized using the Prime Script RT reagent kit (Takara, Beijing, China). Quantitative PCR was performed on a Mini Opticon Real-Time PCR System (Bio-Rad, Hercules, USA) using the SYBR Premix ExTaq (TaKaRa). The expression of four stress responsive genes, including three HSP/chaperones which act as a buffer to limit the misfolding and resolve aggregates under salt and other abiotic stresses (Jacob et al., 2017; Yer et al., 2018) and one respiratory burst oxidase which is involved in the ROS signal transduction response to osmotic and other stresses (Martinière et al., 2019; Wang et al., 2020), were analyzed with *CdSUD1* gene serving as a standard control (Table S1). The relative gene expression level was calculated using the 2^{-ΔΔCt} method (Livak and Schmittgen, 2001). Results of three biological replicates were statistically analyzed by one-way analysis of variance (ANOVA) with Tukey's multiple comparison test.

2.5. Bulk RNA-seq library construction, sequencing and data analyses

Total RNA was extracted from the isolated protoplasts using RNApure Plant kit (Tiangen). RNA integrity and concentration were determined by gel electrophoresis and Nanodrop 2000 spectrophotometer (Thermo Fisher Scientific, Wilmington, USA), respectively. cDNA libraries were prepared using Illumina TruSeq Sample Preparation Kit (Illumina, San Diego, USA) according to the manufacturer's instructions. Agilent 2100 Bioanalyzer (Agilent Technologies, Palo Alto, USA) was used to check the quality of the libraries. The qualified cDNA libraries were paired-end sequenced using Illumina HiSeq™ 3000 (Illumina). Three preparations of protoplasts using leaves collected from different bermudagrass plants were sequenced to represent three replicates. The

sequenced clean reads were aligned to the reference genome of *C. dactylon* cultivar Yangjiang using HISAT2 v2.1.0 (<http://daehwankimlab.github.io/hisat2/>) (Kim et al., 2019; Zhang et al., 2022). The numbers of mapped reads were converted to RPKM (reads per kilobase of transcript per million mapped fragments) values. The \log_2 transformed RPKM values were applied to perform Hierarchical clustering using Pearson's correlation distance in the Pvclust software package (<https://github.com/shimo-lab/pvclust>) with default settings (Suzuki and Shimodaira, 2006).

2.6. scRNA-seq library construction and sequencing

The scRNA-seq libraries were constructed strictly according to the manufacturer's instructions of Chromium Single-Cell 3' Reagent Kit v3.1 (10 \times Genomics, Pleasanton, USA). In brief, the freshly prepared leaf protoplasts with a density of approximately 800 cells/ μ L were loaded into the Chromium microfluidic chips (10 \times Genomics) to generate single cell gel beads. Reverse-transcription reactions were performed to produce barcoded full-length cDNAs, which were PCR amplified using adapter primers to construct the sequencing libraries. The constructed libraries were paired-end sequenced using an Illumina NovaSeq 6000 sequencing system (Illumina) with a sequencing depth of 100,000 reads per cell. Two preparations of protoplasts were sequenced to represent two biological replicates.

2.7. scRNA-seq data processing and cell clustering

The sequencing raw data were converted to FASTQ format using the bcl2fastq2 conversion software v2.20 (Illumina). The Cellranger software v3.1.0 (10 \times Genomics) was used to process the FASTQ files using default parameters. The process included demultiplexing cellular barcodes, aligning map reads to the reference genome, and generating normalized aggregate data across samples. The matrices of gene counts versus cells (output file of Cellranger) were subsequently processed using the R package Seurat v4.2.0 (<https://satijalab.org/seurat/>) (Hao et al., 2021). Low-abundance genes that were expressed in less than three cells, damaged cells in which less than 200 genes were detected, and doublet cells in which more than 6000 genes were detected, were all removed. The filtered expression matrices were normalized using the LogNormalize function. Principal component analysis (PCA) of the scaled data were performed using the RunPCA function. Cell clusters were identified from the principal components using the FindClusters function with a resolution of 0.6. The obtained clusters were visualized using the Uniform Manifold Approximation and Projection (UMAP) algorithm (Becht et al., 2018). The AverageExpression function was used to calculate the average gene expression level of each cluster. Genes differentially expressed across different clusters (DEGs) were detected using the FindMarkers function with default parameters: a Wilcoxon Rank Sum test; above 1.5-fold difference between the two groups of cells; test genes that had a minimum fraction of at least 0.1. The preferentially expressed genes in one cluster were defined as the average gene expression level in this cluster is significantly higher than the average gene expression levels of all other clusters with a \log_2 Fold change >0.25 and p -value <0.05 (Tenorio Berrio et al., 2022).

2.8. RNA in situ hybridization assay

RNA *in situ* hybridization assay was performed as previously described (Wang et al., 2021). Briefly, the middle sections of leaf blades at the 2nd leaf position were harvested and fixed in FAA solution, dehydrated, and embedded in paraffin. The embedded samples were sliced into 7-mm sections and mounted on glass slides. The specific probe sequences of selected target genes (Table S2) were PCR amplified using Pfu DNA polymerase (Sangon Biotech, Shanghai, China) from the cDNA libraries and cloned into the pSPT18 vector. Sense and antisense probes were *in vitro* transcribed using the DIG RNA Labeling Kit (Roche, Mannheim,

Germany) with SP6 and T7 RNA polymerase, respectively. The probes were then applied on leaf sections for hybridization. After washing, the glass slides were incubated with the antidigoxigenin-alkaline phosphatase conjugate (Roche) and visualized by incubation with the nitroblue tetrazolium/5-Bromo-4-chloro-3-indolyl phosphate stock solution (NBT/BCIP solution; Sangon Biotech). The images were then photographed using the Jiangnan BM2000 light microscope (Jiangnan Optics).

2.9. Enzyme activity assay

ME activities were measured following the previously described method (Sonawane et al., 2018). Approximately 1 g of leaf blades was homogenized using a mortar and pestle with ice-cold extraction buffer containing 50 mM HEPES-NaOH (pH 7.8), 5 mM DTT, 5 mM MgCl₂, 1 mM EDTA, 1% (v/v) InStab™ protease inhibitor cocktail (Yeasen Biotechnology, Shanghai, China) and 1% (w/v) polyvinylpyrrolidone. The homogenate was squeezed through three layers of cheesecloth and centrifuged at 12,000 g for 5 min. The obtained supernatant was then used for the protein concentration determination and enzymatic assays. The protein concentration was determined using Bradford method (Bradford, 1976). The NADP-ME activity was measured in assay buffer [50 mM HEPES-NaOH (pH 8.3), 4 mM MgCl₂, 0.5 mM NADP and 0.1 mM EDTA] after the addition of 5 mM malic acid, whereas the NAD-ME activity was measured in assay buffer [50 mM MES-NaOH (pH 6.3), 5 mM DTT, 4 mM MgCl₂, 2 mM NAD, 0.1 mM acetyl-CoA and 0.5 mM EDTA] after the addition of 5 mM malic acid. Activity of the two enzymes was calculated by monitoring the increase of NADPH and NADH absorbance at 340 nm using an Ultrospec 3300 Pro spectrophotometer (Amersham Biosciences, Uppsala, Sweden) with a continuous recording function. One unit (U) of enzyme activity was defined as the amount of enzyme that resulted in the production of 1 μ mol of NADPH/NADH per minute. Three preparations of enzyme extract were assayed to represent three biological replicates.

2.10. Gene ontology enrichment analysis

Gene Ontology (GO) annotation of the DEGs were obtained through BLAST searching against the GO database with an E-value cutoff of 10^{-5} . The R package clusterProfiler (<https://www.bioconductor.org/packages/clusterProfiler>) was then used to perform GO enrichment analysis with default parameters (Wu et al., 2021).

2.11. Weighted gene co-expression network analysis (WGCNA)

The R package hdWGCNA (<https://smorabit.github.io/hdWGCNA/>) was used for WGCNA analysis of the scRNA-seq data following the tutorial instructions (Morabito et al., 2021). The gene co-expression network was visualized using the Cytoscape software v3.9.1 (Shannon et al., 2003).

2.12. Gene family identification and phylogenetic analysis

Protein sequences of the *Arabidopsis* genes were downloaded from the *Arabidopsis* Information Resource (<http://arabidopsis.org/>) and were used as queries to BLAST search against the *C. dactylon* protein database (76,879 sequences, 33, 188, 769 residues) annotated from the genome with an E-value cutoff of 10^{-5} (Zhang et al., 2022). The candidate bermudagrass proteins were further searched against Pfam database (<http://pfam.xfam.org/>) to confirm their identities. The MEGA software v6.0 (<https://megasoftware.net/>) was used to align the amino acid sequences of different gene members belonging to the same gene family. The aligned amino acid sequences were then used to construct the neighbor-joining phylogenetic trees with 1000 bootstrap replicates.

2.13. Gene structure and promoter sequence analyses

Gene structure was constructed using gene structure display server (<http://gsds.gao-lab.org/>) (Hu et al., 2015). The 2000 bp upstream sequences before the gene sequences were selected as gene promoters. Cis-regulatory elements of each promoter sequences were predicted through searching the PlantCARE database (<http://bioinformatics.psb.ugent.be/webtools/plantcare/html/>) with default parameters (Rombauts et al., 1999).

2.14. Yeast one-hybrid assay

The coding sequences of WRKY6 and HsfB1 were PCR amplified from the cDNA and cloned into the pGADT7 expression vector. Genomic DNA was isolated from the harvested leaf blade samples using the Plant DNA Kit (Omega Bio-Tek, Norcross, USA). The 2000 bp promoter fragments of *NADP-ME1* and *NADP-ME2* genes were PCR amplified from the genomic DNA and ligated into the pHIS 2 vector. The primer sequences were listed in Table S1. The sequencing-validated constructs were co-transformed into Y187 yeast cells using the LiAc-PEG method (Gietz et al., 1992). Positive transformants were selected on SD medium lacking tryptophan and leucine (SD-T/L) and grown on SD medium lacking tryptophan, leucine, and histidine (SD-T/L/H) with 2.5 mM 3-amino-1, 2,4-triazole (3-AT) to analyze the binding of transcription factors with promoter sequence.

3. Results

3.1. Bulk RNA-seq and scRNA-seq of bermudagrass leaf blade protoplast population

Leaves of bermudagrass plants are consisted of flat leaf blades and tube-like leaf sheaths surrounding the stems (Fig. 1a). Microscopic analyses indicated that bermudagrass leaf blades have a typical Kranz anatomy of C4 grasses that mesophyll cells are clustered in a ring-like fashion around bundle sheath cells, which further surround the vascular bundle (Fig. 1b–d). Notably, bundle sheath cells have larger cell and vacuole sizes than mesophyll cells, whereas epidermis cells have the smallest cell size (Fig. 1b). Lignin staining further indicated that the vascular bundles are intensely lignified (Fig. 1c), while starch staining revealed that starch were accumulated in the chloroplasts of the bundle sheath cells (Fig. 1d). Using our previously optimized protoplast isolation method, leaf blades were substantially digested (Fig. S1) and protoplast cells possibly representing some different types of bermudagrass leaf blade cells were successfully isolated (Fig. 1e).

Bulk RNA-seq and scRNA-seq libraries were successfully produced from the isolated bermudagrass leaf blade protoplast population, respectively. Gene expression analysis indicated that 49,457 genes were repeatedly detected in bulk RNA-seq libraries (Table S3). Hierarchical clustering analysis revealed that leaf blade protoplast was clustered in one group, whereas other six organs were clustered in another group,

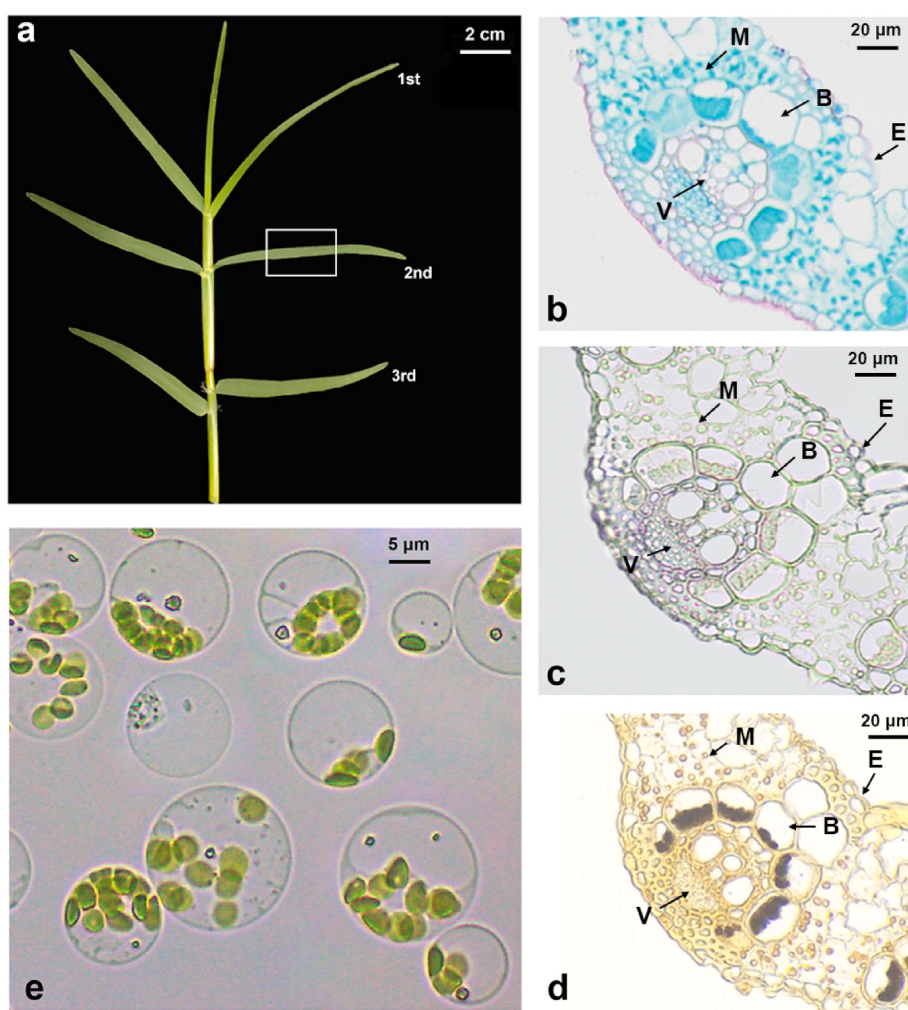


Fig. 1. Cellular characteristics of bermudagrass leaf blades a) Photograph of bermudagrass cultivar Yangjiang showing leaf blades and leaf sheaths. The middle section of leaf blades for sampling was marked using a white rectangle. b) Safranin O-Fast Green, c) Phloroglucinol, and d) I₂-KI staining of the cross section of leaf blades. e) Photograph showing protoplast cells isolated from the leaf blades. Abbreviations: B, bundle sheath; E, epidermis; M, mesophyll; V, vascular bundle.

suggesting their holistic gene expression pattern exhibited massive difference (Fig. S2). The massive gene expression differences between the leaf blade protoplast cell population and the leaf organ might be mainly derived from the enrichment of some cell types during the protoplast preparation step rather than the expression variation of individual genes since the expression levels of selected stress responsive genes all remained stable in the 2 h of protoplast isolation process (Fig. S3). On the other hand, totally 5296 single-cell transcriptomes with an average sequencing depth of 97,127 reads and 8132 unique molecular identifiers per cell were obtained (Table S4). A total of 49,086 genes with a median number of 2664 genes per cell were detected (Tables S4 and S5). Comparison of the gene expression dataset of bulk RNA-seq and the expression matrix of scRNA-seq showed a fine correlation ($R = 0.786$; Fig. S2), suggesting the scRNA-seq data could reveal the expression levels of leaf blade single cells, thus can be used for the downstream analyses. Based on these results, an unsupervised clustering with UMAP analysis was performed on the single-cell transcriptomes to visualize

and explore the cell identities. The analysis result revealed that the bermudagrass leaf blade protoplast population could be grouped into eight distinct cell clusters with different numbers of cells (Fig. 2a; Table S6).

3.2. Identification of different cell types in bermudagrass leaf blades

To determine the identities of different cell clusters, the expression pattern of known marker genes in each cell cluster were analyzed. Genes encoding light-harvesting chlorophyll *a/b*-binding proteins (LHCA and LHCb) all showed high expression level in cluster 1, 2, 5 and 6, especially cluster 2 and 6 (Fig. 2b and S4; Table S7), suggesting these four clusters are different subtypes of mesophyll cells (Broglio et al., 1984). By contrast, the ribulose bisphosphate carboxylase/oxygenase (RuBisCO) small subunit (*RbcS*) gene was specifically expressed in cluster 3 and 4 (Fig. 2b; Table S6), suggesting these two clusters of cells are bundle sheath cells (Bezutczyk et al., 2021). The *early nodulin-like protein 9*

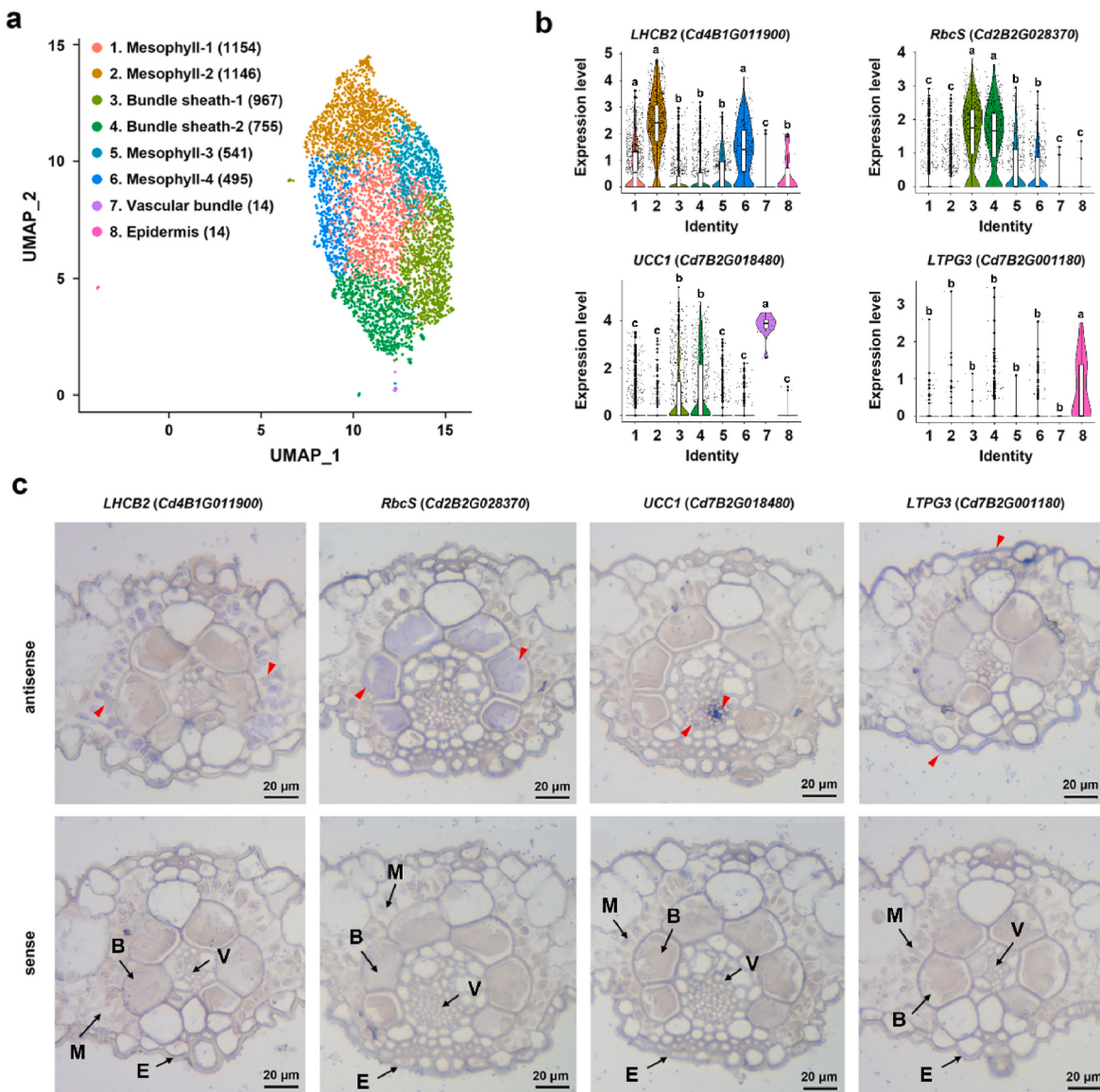


Fig. 2. Cluster analysis of bermudagrass leaf blade cells with representative marker genes. a) UMAP scatterplot of 5296 cells showing the eight cell clusters. Each dot denotes a single cell and different cell clusters are shown with different colors. b) Violin plots showing the normalized expression levels of marker genes encoding light-harvesting chlorophyll *b*-binding protein 2 (LHCb2), ribulose bisphosphate carboxylase small subunit (RbcS), uclacyanin 1 (UCC1), and non-specific lipid transfer protein 3 (LTPG3). Dispersion of the expression values were shown as box plots. Different letters indicate significant differences determined by Wilcoxon Rank Sum test. c) RNA *in situ* hybridization of LHCb2, RbcS, UCC1 and LTPG3 in bermudagrass leaf blades. The positive signals were marked using red triangle. Abbreviations: B, bundle sheath; E, epidermis; M, mesophyll; V, vascular bundle.

(*ENOLD9*) and *uclacyanin 1* (*UCC1*) genes, two marker genes of sieve element and casparyan strips (Khan et al., 2007; Reyt et al., 2020), respectively, were preferentially expressed in cluster 7 (Fig. 2b and S4; Table S6), suggesting this cluster is mainly comprised of vascular bundle cells. Moreover, two genes encoding non-specific lipid transfer proteins (*LTPG3* and *LP1*) were specifically expressed in cluster 8 (Fig. 2b and S4; Table S6), suggesting this cluster of cells are epidermis cells (Tenorio Berrío et al., 2022). RNA *in situ* hybridization assays on selected marker genes confirmed the accuracy of cluster annotations. Specifically, *LHCB2* (*Cd4B1G011900*), *RbcS* (*Cd2B2G028370*), *UCC1* (*Cd7B2G018480*) and *LTPG3* (*Cd7B2G001180*) exhibited specific signals in the mesophyll cell, bundle sheath cell, vascular bundle cell and epidermis cell, respectively (Fig. 2c).

Interestingly, *ferulic acid 5-hydroxylase 1* (*FAH1*), the marker gene of *Arabidopsis* palisade mesophyll cells (Procko et al., 2022), was preferentially expressed in cluster 2 and 6 (Fig. S4), suggesting these subtypes of bermudagrass mesophyll cells might behave like palisade cells, whereas another two clusters of mesophyll cells (cluster 1 and 5) might

behave like spongy cells. Accordingly, genes involved in light reactions of photosynthesis, including *LHCA* and *LHCB*, as well as *Photosystem II reaction center w* (*PSBW*), all showed higher expression levels in these ‘palisade-like’ mesophyll cells (Fig. S4). Notably, the two clusters of ‘palisade-like’ mesophyll cells also showed significant gene expression variance. For example, both *plastid ribosomal proteins of the 50S subunit 5* (*PRPL5*) and *protochlorophyllide oxidoreductase a* (*PORA*) genes were highly expressed in cluster 6 but weakly expressed in cluster 2 (Fig. S4). Similar variation of gene expression could also be found between the two ‘spongy-like’ mesophyll cells that *phospholipid sterol acyl transferase 1* (*PSAT1*) and *beta-amylase 1* (*BAM1*) genes were both preferentially expressed in cluster 5 (Fig. S4). On the other hand, gene expression in the two clusters of bundle sheath cell also displayed significant differences. For example, the *NAD(P)-linked oxidoreductase superfamily protein* (*NDH1*) gene was preferentially expressed in cluster 3, whereas the *sugar transporter 1* (*STP1*) gene was preferentially expressed in cluster 4 (Fig. S4).

Differential expression of C4 photosynthesis-related genes in

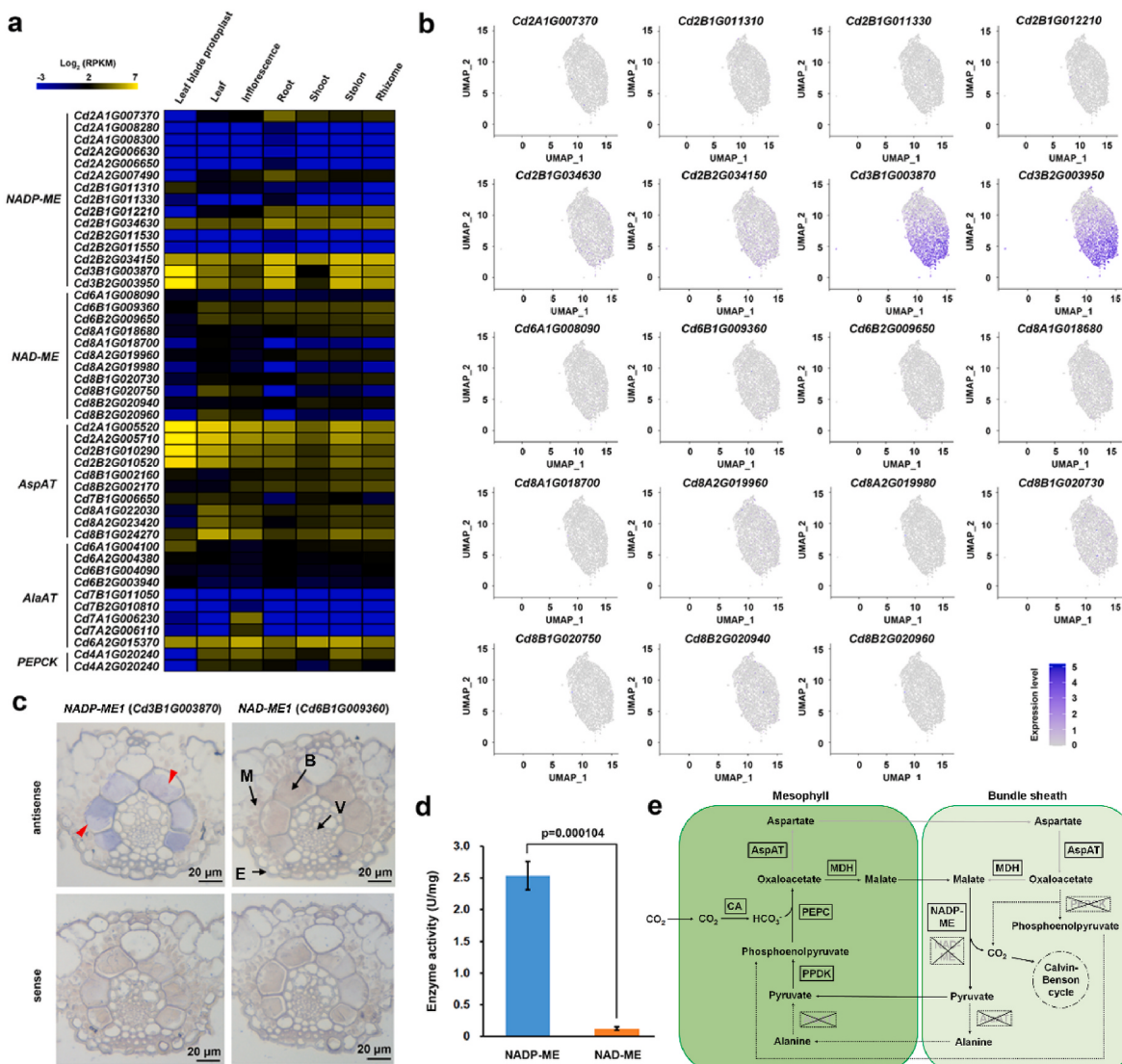


Fig. 3. C4 photosynthesis in bermudagrass leaf blades a) Heatmap showing the expression levels of different C4 photosynthesis-related genes in leaf blade protoplasts and six organs of bermudagrass cultivar Yangjiang through bulk RNA-seq analyses. b) Feature plots showing the normalized expression levels of 19 ME genes in bermudagrass leaf blades. c) RNA *in situ* hybridization of NADP-ME4 and NAD-ME1 genes in bermudagrass leaf blades. The positive signals were marked using red triangle. Abbreviations: B, bundle sheath; E, epidermis; M, mesophyll; V, vascular bundle. d) Malic enzyme activity of bermudagrass leaf blades. e) Diagram showing the possible C4 photosynthetic pathway in bermudagrass leaf blades. The existent and absent routes are marked with solid (black color: malate route with enzymatic evidence, grey color: aspartate route without enzymatic evidence) and dashed arrows, respectively.

mesophyll and bundle sheath cells of bermudagrass leaf blades.

Phosphoenolpyruvate carboxylase (PEPC) and pyruvate, phosphate dikinase (PPDK), two C4 photosynthesis-related enzymes known to function in mesophyll cells (Chang et al., 2012), were all highly expressed in the four clusters of mesophyll cells (Fig. S4; Table S8). By contrast, two genes encoding chloroplastic NADP-ME, another C4 photosynthesis-related enzyme that functions in bundle sheath cells, showed preferential expression in the two clusters of bundle sheath cells (Fig. S4; Table S8). Interestingly, there are totally 15 NADP-ME and 11 NAD-ME genes in bermudagrass (Fig. S5). Previous organ-specific transcriptomics analysis revealed that 8 NADP-ME genes and 11 NAD-ME genes were significantly expressed ($RPKM > 1$) in bermudagrass leaves (Fig. 3a) (Chen et al., 2021), however, current bulk RNA-seq and scRNA-seq dataset collectively indicated that only the two above-mentioned chloroplastic NADP-ME genes (*Cd3B1G003870* and *Cd3B2G003950*) were highly expressed in leaf blades whereas other NADP-ME genes and all the NAD-ME genes were weakly expressed in a few cells (Fig. 3a and b). In line with these results, RNA *in situ* hybridization assays showed that NADP-ME1 (*Cd3B1G003870*) exhibits specific signals in bundle sheath cells, whereas NAD-ME1 (*Cd6B1G009360*) was scarcely detected in all cells (Fig. 3c). Furthermore, enzyme activity measurements also indicated that NADP-ME activity was 16-fold higher than that of NAD-ME in leaf blades (Fig. 3d). In combination with the observation that phosphoenolpyruvate carboxykinase (PCK) genes were not detected in the scRNA-seq libraries (Fig. S5; Table S8), these results collectively implied that bermudagrass might be a NADP-ME type of C4 grass (Fig. 3e). Interestingly, four chloroplastic aspartate aminotransferase (ASP) genes possibly participating in the shuttle of C4 acids between mesophyll and bundle sheath cells were highly expressed in all cell clusters, whereas alanine aminotransferase genes that are involved in the shuttle of C3 acids were weakly expressed in a few cells (Figs. S5

and S6; Table S8).

Starch synthesis and degradation was preferentially regulated in different cell types of bermudagrass leaf blades.

Based on the DEG analysis results, genes preferentially expressed in each cluster of cells were successfully captured (Fig. 4a; Table S6). GO enrichment analysis indicated that genes preferentially expressed in cluster 2 and 6 were enriched in light reaction of photosynthesis pathway, which is in line with the canonical function of these ‘palisade-like’ mesophyll cells (Fig. 4b; Table S9). Genes preferentially expressed in cluster 3 were enriched in glutathione metabolic process, whereas genes preferentially expressed in cluster 4 were enriched in proteolysis and glycolysis, suggesting the two subtypes of bundle sheath cells have different metabolic activities (Fig. 4b; Table S9). By contrast, genes highly expressed in cluster 7 (vascular bundle) were enriched in xyloglucan and chitin metabolic process (Fig. 4b; Table S9). Interestingly, genes highly expressed in cluster 3 and 4 (bundle sheath) were enriched in starch metabolic process, whereas genes preferentially expressed in cluster 5 (mesophyll) were enriched in polysaccharide catabolic process (Fig. 4b; Table S9), which is in accord with the I₂-KI staining result that starch were specifically accumulated in bundle sheath cells (Fig. 1d).

To further explore the regulation mechanism of starch metabolism in bermudagrass leaf blades, the expression of genes participating in the synthesis and degradation of starch were systematically analyzed at the single-cell level (Bahaji et al., 2014) (Fig. 4c; Table S10). The results indicated that key enzymes required for the synthesis of starch, including glucose-1-phosphate adenylyltransferase (AGPase), starch synthase (SS) and 1,4-alpha-glucan-branched enzyme (SBE), were highly expressed in bundle sheath cells (cluster 3 and 4). By contrast, BAM, key enzyme involved in the degradation of starch, showed high expression level in mesophyll cells (cluster 5 and 6) (Fig. 4d). In accord with these results, RNA *in situ* hybridization assays revealed that SS4

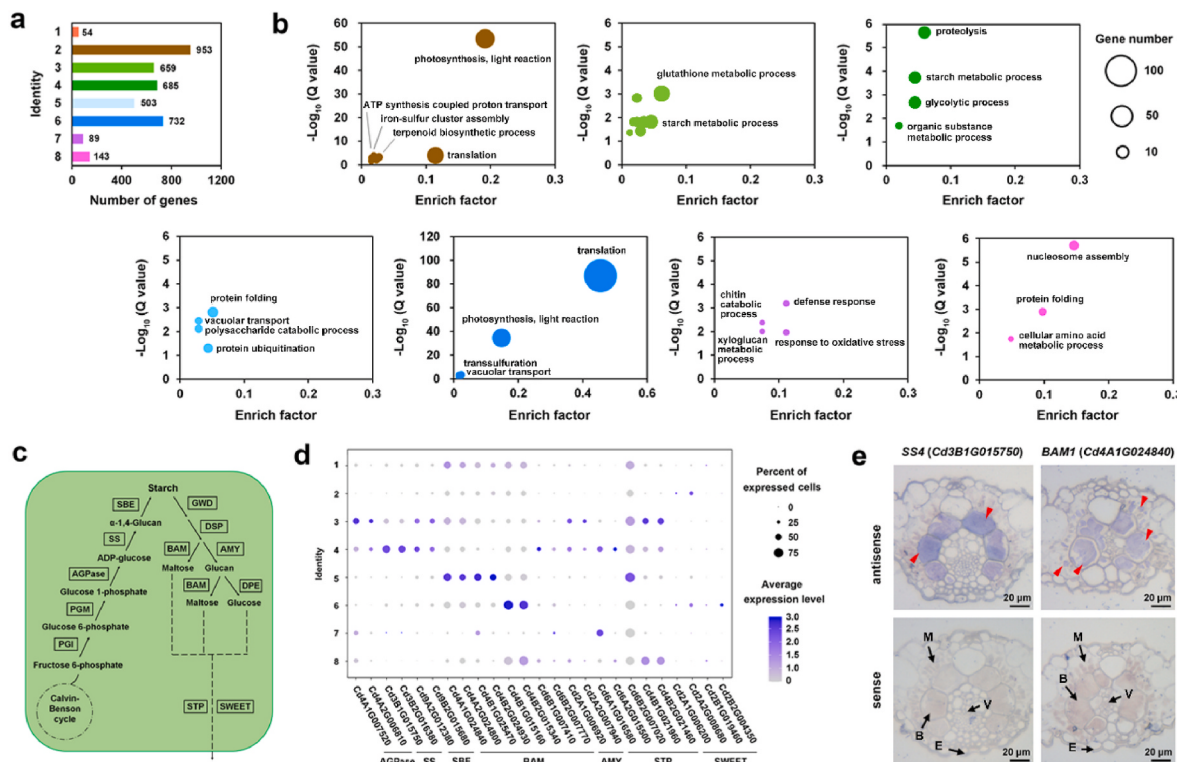


Fig. 4. Functional diversity of different cell types in bermudagrass leaf blades a) Numbers of genes preferentially expressed in the eight cell clusters. b) Biological processes significantly enriched with preferentially expressed genes (DEGs) in different cell clusters. Node size corresponds to the number of DEGs. c) Diagram showing the possible starch metabolic pathway in bermudagrass leaf blades. d) Dotplot showing the average expression levels of key starch metabolic genes in the eight cell clusters. e) RNA *in situ* hybridization of *SS4* and *BAM1* genes in bermudagrass leaf blades. The positive signals were marked using red triangle. Abbreviations: AGPase, Glucose-1-phosphate adenylyltransferase; SS, Starch synthase; SBE, 1,4-alpha-glucan-branched enzyme; BAM, Beta-amylase; AMY, Alpha-amylase; STP, Sugar transport protein; SWEET, Bidirectional sugar transporter; B, bundle sheath; E, epidermis; M, mesophyll; V, vascular bundle.

(*Cd3B1G015750*) exhibits specific signals in bundle sheath cells, whereas *BAM1* (*Cd4A1G024840*) showed strong signals in both bundle sheath cells and mesophyll cells (Fig. 4e). Interestingly, sugar transport protein (STP) and bidirectional sugar transporter (SWEET), two types of transporter proteins responsible for the exchange of saccharides between cells, showed different expression patterns among the different cell types. Specifically, one *STP* gene (*Cd6B2G007020*) was highly expressed in cluster 5 (mesophyll), two *STP* genes (*Cd4B1G021960* and *Cd4B2G021460*) were highly expressed in cluster 3 (bundle sheath) and cluster 8 (epidermis), whereas the four *SWEET* genes (*Cd2A1G006200*, *Cd2A2G008680*, *Cd2B1G019460* and *Cd2B2G004350*) were all weakly expressed in cluster 2 and 6 (mesophyll) and scarcely detected in bundle sheath cells (Fig. 4d). These results collectively implied that soluble sugar content was strictly regulated in bermudagrass leaf blades.

3.3. Putative transcription regulatory network of the C4 photosynthesis in bermudagrass leaf blades

WGCNA of the scRNA-seq data successfully identified 12 gene modules with different numbers of genes (Fig. S7). Interestingly, genes involved in the C4 photosynthesis, including 20 genes encoding different light-harvesting chlorophyll *a/b*-binding proteins (LHCA and LHCb) as well as the highly expressed *PEPC*, *PPDK*, *ASP* and *NADP-ME* genes, were all clustered in the same module (color turquoise with 2608 genes). Notably, 42 TFs belonging to different TF families, including *G2-Like*, *bHLH*, *bZIP*, *HSF* and *WRKY*, were also identified in this module. The functional genes and the co-expressed transcription factors collectively form a putative transcription regulatory network of the C4 photosynthesis (Fig. S7; Table S11).

To further characterize the possible regulatory functions of different TFs in the C4 photosynthesis of bermudagrass leaf blades, the expression of the TFs were also systematically analyzed at the single-cell level (Fig. 5a; Table S12). The results indicated that *GLK2* (*Cd7A2G013110*), *PIF4* (*Cd2A2G018740*), *bHLH104* (*Cd8B1G029750*), *GBF2* (*Cd3A1G012110*) and *WRKY54* (*Cd3B2G005940*) were highly expressed in mesophyll cells (cluster 1, 2, 5 and 6, especially 2 and 6), whereas *bZIP22* (*Cd6A2G000660*), *HsfB1* (*Cd7B1G010050*), *HsfB2b* (*Cd7A1G010580*), *HsfB3* (*Cd7B2G009810*), *WRKY6* (*Cd2A2G031900*) and *NFYC11* (*Cd1A1G003150*) were preferentially expressed in bundle sheath cells (cluster 3 and 4). In line with these results, cis-regulatory element analysis indicated that promoters of *PEPC* and *PPDK* genes that were highly expressed in mesophyll cells have several G-box elements, which could be bound by TFs from *bZIP* and *bHLH* families (Ezer et al., 2017) (Fig. S8). By contrast, promoters of *NADP-ME* genes that were highly expressed in bundle sheath cells simultaneously have G-box, W box, and HSE elements, which could be bound by *bZIP*, *bHLH*, *WRKY* and *HSF* families of TFs (Birkenbihl et al., 2018; Guertin and Lis, 2010) (Fig. S8). In line with these observations, yeast one-hybrid assays indicated that *WRKY6* and *HsfB1*, two TFs preferentially expressed in bundle sheath cells, could bind to the promoters of the two *NADP-ME* genes (Fig. 5b). These results, in combination with the WGCNA results, collectively suggested that two distinct transcription regulatory networks consisting of different TFs and functional genes might exist in mesophyll and bundle sheath cells to synergistically regulate the expression of key enzymes in different cells to drive the efficient operation of C4 photosynthesis in bermudagrass leaf blades (Fig. 5c).

4. Discussion

ScRNA-seq analysis identified four subtypes of mesophyll, two subtypes of bundle sheath, as well as epidermis and vascular bundle cells in bermudagrass leaf blades.

As a typical warm-season turfgrass species, bermudagrass grows quickly at sunny days of summer and autumn in tropical and subtropical areas because of the existence of the C4 photosynthetic pathway (Xu et al., 2022; Zhang et al., 2018). To maximize the absorption of sun light,

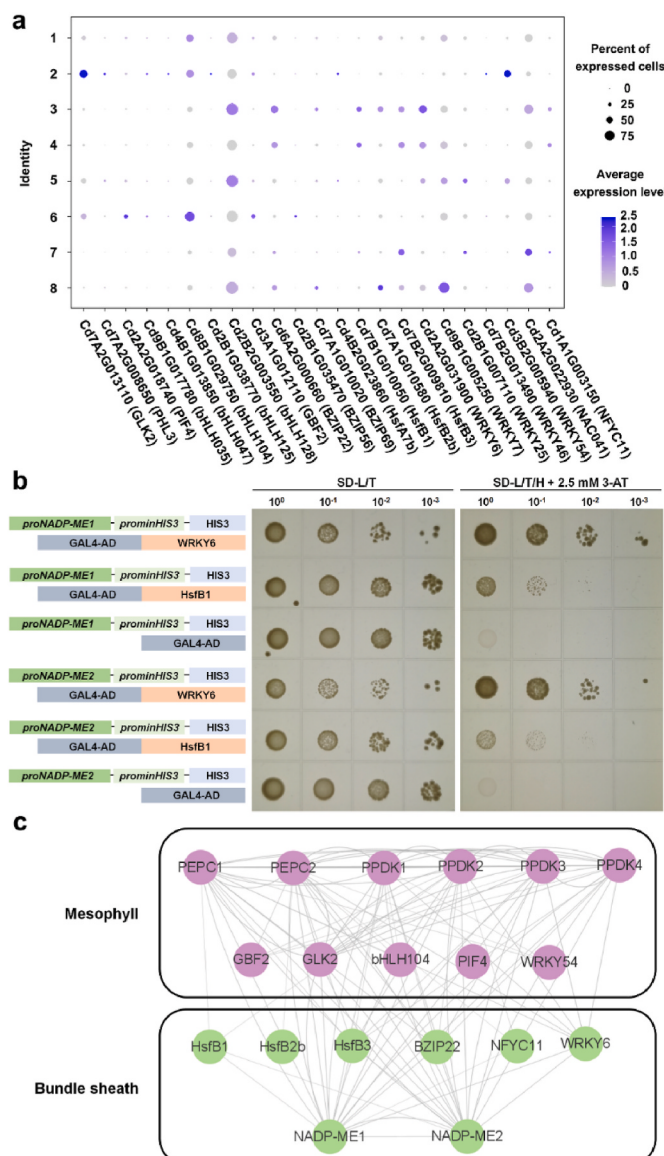


Fig. 5. Transcription factors possibly involved in C4 photosynthesis in bermudagrass leaf blades a) Dotplot showing the average expression levels of key TFs in the eight cell clusters. b) Yeast one-hybrid assay of the binding of *WRKY6* and *HsfB1* with the promoter sequences of *NADP-ME1* and *NADP-ME2*. Left panel, diagram showing the constructs co-transformed into the yeast cells; Right panel, growth phenotype of different yeast cells. c) Transcription regulation network consisting of different TFs and functional genes in mesophyll and bundle sheath cells.

leaves of bermudagrass plants are thin and flat (Fig. 1a). Similar to other C4 plants, leaf blades of bermudagrass plants also have the typical Kranz anatomy that mesophyll cells and bundle sheath cells are distributed in an orderly arrangement (Furbank, 2017) (Fig. 1b-d). Using scRNA-seq, a total of 5296 protoplast cells isolated from the bermudagrass leaf blades were successfully grouped into eight distinct cell clusters (Fig. 2). Through assigning the cell identities with known marker genes, 99.47% of cells were found to be mesophyll cells (3336 cells) and bundle sheath cells (1722 cells), whereas only 28 cells were identified as epidermis and vascular bundle cells (Fig. 2). By contrast, previous scRNA-seq analysis of Arabidopsis and rice leaves both identified more than ten distinct cell types including hundreds of epidermis and vasculature cells (Tenorio Berrio et al., 2022; Wang et al., 2021). We suspect the low ratio of epidermis and vascular bundle cells in the bermudagrass leaf blade protoplast populations was possibly derived from the deficiency of

protoplast preparation process since majority of epidermis were torn out from the leaf blades during protoplast preparation procedures while vascular bundles, even bundle sheath, almost remained undigested in the 2 h of enzymatic digestion process (Fig. S1) (Chen et al., 2023). Because the cell number of epidermis and vascular bundle cells was too small, stomata and trichome cells of epidermis and specific types of vascular bundle cells could not be discriminated in the following scRNA-seq analyses. Unsurprisingly, similar low ratio of epidermis and vascular bundle cells (72/7354, 0/3242) was also observed in the scRNA-seq analysis of leaves in maize, a C4 grass species with similar leaf shape and anatomy as bermudagrass does (Tao et al., 2022; Bezrutczyk et al., 2021). Further improvement of the protoplast preparation method might increase the types of cells, especially the different types of vascular bundle cells, in the scRNA-seq analysis result. However, considering that the gene expression levels were significantly changed after long time of enzymatic digestion (>4 h) (Fig. S3), elevation of enzymatic digestion efficacy rather than elongation of digestion time should be the focus of future experiments (Edwards et al., 2001).

Owing to its high sensitivity and specificity, scRNA-seq could distinguish different subpopulations belonging to the same cell types that might be imperceptible in bulk RNA-seq (Islam et al., 2024). In Arabidopsis, four and seven subtypes of mesophyll cells were identified by two scRNA-seq analyses, respectively (Procko et al., 2022; Tenorio Berrío et al., 2022). ScRNA-seq analysis also identified five subtypes of mesophyll cells and two subtypes of bundle sheath cells in maize (Bezrutczyk et al., 2021). Through scRNA-seq analysis, four subtypes of mesophyll cells and two subtypes of bundle sheath cells were also successfully discriminated in bermudagrass leaf blades (Fig. 2). Interestingly, the four subtypes of mesophyll cells could be divided into two groups, the ‘palisade-like’ and ‘spongy-like’ mesophyll cells, each containing two clusters of cells (Fig. S4). In dicot plants, the columnar palisade mesophyll cells are located below the upper epidermis and have a high photosynthetic rate, whereas the irregular and loosely packed spongy mesophyll cells position below the palisade cells and mainly function in scattering light and promoting CO₂ diffusion from the stomata to the palisade cells (Borsuk et al., 2022). The ‘palisade-like’ and ‘spongy-like’ mesophyll cells in bermudagrass leaf blades might have similar functional differentiation since genes involved in light reactions of photosynthesis were all preferentially expressed in the ‘palisade-like’ mesophyll cells (Figs. S4 and 4b). Similar to the leaves of Arabidopsis and maize, bermudagrass leaves also have upper (adaxial) and lower (abaxial) sides (Fukushima and Hasebe, 2014). The two subtypes of bundle sheath cells as well as the ‘palisade-like’ and ‘spongy-like’ mesophyll cells might reflect the adaxial and abaxial differentiation of these cells. In line with this suspicion, *NDH1* gene and other *NDH* genes, which are involved in the formation of bundle sheath thylakoid NDH complex (Majeran and van Wijk, 2009), were all preferentially expressed in cluster 3 (Fig. S4; Table S6). By contrast, *STP1* genes participating in the transport of sugars were preferentially expressed in cluster 4 (Fig. S4; Table S6). Considering that abaxial bundle sheath cells of maize was enriched with transport proteins (Bezrutczyk et al., 2021), these results implied that cluster 4 might be the abaxial bundle sheath cells.

ScRNA-seq analysis suggested bermudagrass might be a NADP-ME type C4 plant.

C4 photosynthesis has independently evolved over 66 times in 19 families of the plant kingdoms (Sage, 2017). Through spatial separation of initial CO₂ fixation in mesophyll cells and subsequent refixation by RuBisCO in bundle sheath cells, C4 photosynthesis could partially overcome the catalytic inefficiency of RuBisCO and reduce the energy cost in photorespiration, thereby providing competitive edges to C4 plants (Furbank and Kelly, 2021). Depending on the enzymes catalyzing the decarboxylation reactions in bundle sheath cells, C4 pathways are classified into three classical types: NADP-ME type, NAD-ME type and PCK type. Previous enzymatic analysis reported that NAD-ME activity was higher than NADP-ME activity in bermudagrass leaves, suggesting

bermudagrass has a NAD-ME type of C4 photosynthesis (Hatch and Kagawa, 1974). However, scRNA-seq analysis clearly indicated that only two *NADP-ME* genes were highly expressed in bundle sheath cells of bermudagrass leaf blades, whereas all the *NAD-ME* genes were weakly expressed in the eight cell clusters, which was supported by the RNA *in situ* hybridization assay of two different types of *ME* genes (Fig. 3b and c). Moreover, enzyme activity assay results further indicated that NADP-ME activity was much higher than that of NAD-ME in bermudagrass leaf blades (Fig. 3d). These results strongly suggested that bermudagrass might have a NADP-ME type of C4 photosynthesis pathway (Fig. 3e). ScRNA-seq analysis also indicated that *ASP* genes were highly expressed in both mesophyll and bundle sheath cells (Fig. S6), suggesting that aspartate might be used as a supplement to the malate for shuttling between the mesophyll and bundle sheath cells. Similar atypical NADP-ME type of C4 photosynthesis pathway using both malate and aspartate as the transferred C4 acids was also observed in maize (Bellasio and Griffiths, 2014; Ludwig, 2016), however, more experiment evidences are required to elucidate the existence of aspartate route in bermudagrass (Fig. 3e). It is noteworthy that the two *NADP-ME* genes were also highly expressed in epidermal and vascular bundle cells (Fig. S4; Table S8). Similar high expression of *NADP-ME* in these two cell types was also observed in maize (Tao et al., 2022). These results collectively suggested that the expression of *NADP-ME* genes might adhere to a negative regulation mechanism that its expression was specifically inhibited in mesophyll cells rather than simply elevated in bundle sheath cells. On the other hand, it is also noteworthy that four *NAD-ME* genes were substantially expressed in bermudagrass leaves (Fig. 3a). Considering that the organ-specific transcriptome analysis sampled the whole bermudagrass leaf including leaf blade and leaf sheath (Chen et al., 2021), this result implied that these *NAD-ME* genes might be highly expressed in the leaf sheath of bermudagrass, which is understandable because over 60% genes were differently expressed along the leaf vein of maize leaves (Li et al., 2010). Since the previous study observed relatively high NAD-ME activity in bermudagrass leaves (Hatch and Kagawa, 1974), systematic comparison of NADP-ME and NAD-ME activities in different leaves as well as single cell metabolome analysis of different leaf cell types may need to be performed in the future to accurately determine which type of C4 pathway majorly works in bermudagrass.

ScRNA-seq analysis revealed the sugar metabolism difference in mesophyll and bundle sheath cells of bermudagrass leaf blades.

Except functional divergence in C4 photosynthesis, mesophyll and bundle sheath cells of bermudagrass leaf blades also showed different activities in other biological processes, especially the starch metabolic process (Fig. 4b). In agreement with the previous report that bermudagrass is a starch-accumulating plant (Miyake and Maeda, 1978), chloroplasts filled with starch were clearly visible in bundle sheath cells of bermudagrass leaf blades under microscopy (Fig. 1d). Accordingly, scRNA-seq analysis indicated that starch synthesis-related genes were preferentially expressed in bundle sheath cells, whereas starch degradation-related *BAM* genes were highly expressed in mesophyll cells, which was supported by the RNA *in situ* hybridization assay of *SS4* and *BAM1* genes (Fig. 4d and e). Similar preferential expression of starch synthesis-related genes in bundle sheath cells and high expression of *BAM6* and *DSP4* genes in mesophyll cells were also observed in maize (Majeran et al., 2005; Friso et al., 2010). These results further provided evidence to the suspicion that enzymes involved in starch biosynthesis preferentially accumulate in the bundle sheath cells of all C4 plants under normal growth conditions (Furbank and Kelly, 2021). By contrast, synergistic low expression of enzymes involved in starch synthesis and high expression of enzymes for starch degradation might aid to the accumulation of sucrose rather than starch in mesophyll cells. Interestingly, sugar transport proteins, which are required for the exchange of solute sugars among different cells, showed cell-type-specific expression patterns (Fig. 4d). Different members of sugar transport protein families play important roles in the distribution of photoassimilates among

different cells of leaf blades and transportation of photoassimilates to other organs through vascular systems (Slewinski, 2011; Dhungana and Braun, 2021). In maize, three SWEET proteins are highly expressed in the abaxial bundle sheath cells to facilitate the translocation of sucrose to sieve elements of the companion cells, the so-called phloem loading process (Bezrutczyk et al., 2021). However, the SWEET genes were almost not expressed in bundle sheath cells of bermudagrass leaf blades, whereas two STP genes were highly expressed in these cells (Fig. 4d). These results implied that bermudagrass might use STP rather than SWEET for phloem loading.

ScRNA-seq analysis revealed possible transcription regulatory networks in mesophyll and bundle sheath cells of bermudagrass leaf blades.

The anatomical, biochemical and functional heterogeneity of mesophyll and bundle sheath cells is derived from the gene expression difference, which in turn is resulted from differential transcription regulation of the same set of genes (Hibberd and Covshoff, 2010). In the past several years, a few studies have successfully identified many TFs possibly involved in the differentiation of mesophyll and bundle sheath cells. For example, comparative transcriptome analysis of rice and maize leaves identified the possible transcription regulators of maize C4 enzymes, whereas genome-wide sequencing on mesophyll and bundle sheath cells isolated from maize leaves identified 25 WRKY and 12 Dof TFs with different expression levels between the two cell types (Chang et al., 2019; Dai et al., 2022). Similarly, WGCNA analysis of the scRNA-seq data generated in the current study successfully identified 42 TFs co-expressing with the functional genes of C4 photosynthesis in bermudagrass leaf blades (Fig. S7). Expression profiling further indicated that five TFs were highly expressed in mesophyll cells, whereas other six TFs were preferentially expressed in bundle sheath cells (Fig. 5a). Interestingly, functional genes highly expressed in mesophyll cells and bundle sheath cells have different TF binding cis-regulatory elements in the promoter region, respectively (Fig. S8). Yeast one-hybrid assays confirmed the binding of two TFs, WRKY6 and HsfB1, with the promoters of NADP-ME genes (Fig. 5b), implying that the two TFs might contribute to the relatively high expression of the two NADP-ME genes in bundle sheath cells. Collectively, these results implied that two distinct transcription regulatory networks consisting of different TFs and functional genes might exist in mesophyll and bundle sheath cells of bermudagrass leaf blades to synergistically regulate the C4 photosynthesis (Fig. 5c). In the future, systematic interaction analysis of TFs with the promoters of functional genes containing the corresponding cis-regulatory elements through yeast one-hybrid assays as well as in-depth analysis of the genetic relationships between the TFs and functional genes by transgenic experiments could be conducted to characterize the detailed regulation mechanism of the transcription regulatory networks.

5. Conclusion

In summary, we preliminarily analyzed the gene expression atlas of bermudagrass leaf blades at single-cell resolution. Different cell clusters corresponding to four subtypes of mesophyll, two subtypes of bundle sheath, as well as epidermis and vascular bundle cells were identified. An atypical NADP-ME type of C4 pathway was depicted, whereas different functions of mesophyll and bundle sheath cells in starch metabolism were also explored. WGCNA and gene expression profiling further identified five and six TFs possibly involved in the transcriptional regulation of C4 enzymes in mesophyll and bundle sheath cells, respectively. These results collectively expanded our understanding of C4 photosynthesis regulation in bermudagrass.

Funding

This study was financially supported by the National Natural Science Foundation of China (32072613).

CRediT authorship contribution statement

Bing Zhang: Writing – review & editing, Writing – original draft, Validation, Supervision, Investigation, Funding acquisition, Data curation, Conceptualization. **Ziyan Ma:** Investigation. **Hailin Guo:** Writing – review & editing, Resources, Investigation. **Si Chen:** Software, Methodology, Investigation, Data curation. **Jianxiu Liu:** Writing – review & editing, Resources, Investigation.

Declaration of competing interest

The authors declare that they have no known competing financial interests or personal relationships that could have appeared to influence the work reported in this paper.

Data availability

Bulk RNA-seq and scRNA-seq raw sequencing data generated in this work have been submitted to the SRA database at NCBI under the Bio-Project accession number PRJNA1045520 and PRJNA918429, respectively.

Acknowledgements

The authors want to thank the Novogene Corporation and Servicebio Technology Corporation for the technical assistances in scRNA-seq analysis and *in situ* hybridization experiments, respectively.

Appendix A. Supplementary data

Supplementary data to this article can be found online at <https://doi.org/10.1016/j.plaphy.2024.108857>.

References

- Bahaji, A., Li, J., Sánchez-López, Á.M., Barroja-Fernández, E., Muñoz, F.J., Ovecka, M., Almagro, G., Montero, M., Ezquer, I., Etxeberria, E., Pozueta-Romero, J., 2014. Starch biosynthesis, its regulation and biotechnological approaches to improve crop yields. *Biotechnol. Adv.* 32, 87–106.
- Bai, Y., Liu, H., Lyu, H., Su, L., Xiong, J., Cheng, Z.M., 2022. Development of a single-cell atlas for woodland strawberry (*Fragaria vesca*) leaves during early *Botrytis cinerea* infection using single cell RNA-seq. *Hortic. Res.* 9, uhab055.
- Becht, E., McInnes, L., Healy, J., Dutertre, C.A., Kwok, I.W.H., Ng, L.G., Ginhoux, F., Newell, E.W., 2018. Dimensionality reduction for visualizing single-cell data using UMAP. *Nat. Biotechnol.* 37, 38–44.
- Bellasio, C., Griffiths, H., 2014. The operation of two decarboxylases, transamination, and partitioning of C4 metabolic processes between mesophyll and bundle sheath cells allows light capture to be balanced for the maize C4 pathway. *Plant Physiol.* 164, 466–480.
- Bezrutczyk, M., Zöllner, N.R., Kruse, C.P.S., Hartwig, T., Lautwein, T., Köhrer, K., Frommer, W.B., Kim, J.Y., 2021. Evidence for phloem loading via the abaxial bundle sheath cells in maize leaves. *Plant Cell* 33, 531–547.
- Borsuk, A.M., Roddy, A.B., Théroux-Rancourt, G., Brodersen, C.R., 2022. Structural organization of the spongy mesophyll. *New Phytol.* 234, 946–960.
- Bradford, M.M., 1976. A rapid and sensitive method for the quantitation of microgram quantities of protein utilizing the principle of protein-dye binding. *Anal. Biochem.* 72, 248–254.
- Birkenbihl, R.P., Kracher, B., Ross, A., Kramer, K., Finkemeier, I., Somssich, I.E., 2018. Principles and characteristics of the *Arabidopsis* WRKY regulatory network during early MAMP-triggered immunity. *Plant J.* 96, 487–502.
- Broglie, R., Coruzzi, G., Keith, B., Chua, N.H., 1984. Molecular biology of C4 photosynthesis in Zea mays: differential localization of proteins and mRNAs in the two leaf cell types. *Plant Mol. Biol.* 3, 431–444.
- Chang, Y.M., Lin, H.H., Liu, W.Y., Yu, C.P., Chen, H.J., Wartini, P.P., Kao, Y.Y., Wu, Y.H., Lin, J.J., Lu, M.J., Tu, S.L., Wu, S.H., Shiu, S.H., Ku, M.S.B., Li, W.H., 2019. Comparative transcriptomics method to infer gene coexpression networks and its applications to maize and rice leaf transcriptomes. *Proc Natl Acad Sci U S A* 116, 3091–3099.
- Chang, Y.M., Liu, W.Y., Shih, A.C., Shen, M.N., Lu, C.H., Lu, M.Y., Yang, H.W., Wang, T.Y., Chen, S.C., Chen, S.M., Li, W.H., Ku, M.S., 2012. Characterizing regulatory and functional differentiation between maize mesophyll and bundle sheath cells by transcriptomic analysis. *Plant Physiol* 160, 165–177.
- Chen, S., Liu, J., Zhang, B., 2023. Efficient leaf mesophyll protoplast isolation and transient gene expression in bermudagrasses (*Cynodon* spp.). *Plant Cell Tissue Organ Cult.* 152, 229–235.

- Chen, S., Xu, X., Ma, Z., Liu, J., Zhang, B., 2021. Organ-specific transcriptome analysis identifies candidate genes involved in the stem specialization of bermudagrass (*Cynodon dactylon* L.). *Front. Genet.* 12, 678673.
- Chen, T.M., Brown, R.H., Black, C.C., 1969. Photosynthetic activity of chloroplasts isolated from bermudagrass (*Cynodon dactylon* L.), a species with a high photosynthetic capacity. *Plant Physiol.* 44, 649–654.
- Dai, X., Tu, X., Du, B., Dong, P., Sun, S., Wang, X., Sun, J., Li, G., Lu, T., Zhong, S., Li, P., 2022. Chromatin and regulatory differentiation between bundle sheath and mesophyll cells in maize. *Plant J.* 109, 675–692.
- Dhungana, S.R., Braun, D.M., 2021. Sugar transporters in grasses: function and modulation in source and storage tissues. *J. Plant Physiol.* 266, 153541.
- Edwards, G.E., Franceschi, V.R., Ku, M.S., Voznesenskaya, E.V., Pyankov, V.I., Andreo, C.S., 2001. Compartmentation of photosynthesis in cells and tissues of C4(4) plants. *J. Exp. Bot.* 52, 577–590.
- Ermakova, M., Danila, F.R., Furbank, R.T., von Caemmerer, S., 2020. On the road to C4 rice: advances and perspectives. *Plant J.* 101, 940–950.
- Ezer, D., Shepherd, S.J.K., Bretovitsky, A., Dickinson, P., Cortijo, S., Charoensawan, V., Box, M.S., Biswas, S., Jaeger, K.E., Wigge, P.A., 2017. The G-box transcriptional regulatory code in *Arabidopsis*. *Plant Physiol.* 175, 628–640.
- Fernández-Marín, B., Gulías, J., Figueroa, C.M., Iñiguez, C., Clemente-Moreno, M.J., Nunes-Nesi, A., Fernie, A.R., Cavieres, L.A., Bravo, L.A., García-Plazaola, J.I., Gago, J., 2020. How do vascular plants perform photosynthesis in extreme environments? An integrative ecophysiological and biochemical story. *Plant J.* 101, 979–1000.
- Frisco, G., Majeran, W., Huang, M., Sun, Q., van Wijk, K.J., 2010. Reconstruction of metabolic pathways, protein expression, and homeostasis machineries across maize bundle sheath and mesophyll chloroplasts: large-scale quantitative proteomics using the first maize genome assembly. *Plant Physiol.* 152, 1219–1250.
- Fukushima, K., Hasebe, M., 2014. Adaxial-abaxial polarity: the developmental basis of leaf shape diversity. *Genesis* 52, 1–18.
- Furbank, R.T., 2017. Walking the C4 pathway: past, present, and future. *J. Exp. Bot.* 68, 4057–4066.
- Furbank, R.T., Kelly, S., 2021. Finding the C4 sweet spot: cellular compartmentation of carbohydrate metabolism in C4 photosynthesis. *J. Exp. Bot.* 72, 6018–6026.
- Gietz, D., St Jean, A., Woods, R.A., Schiestl, R.H., 1992. Improved method for high efficiency transformation of intact yeast cells. *Nucleic Acids Res.* 20, 1425.
- Guertin, M.J., Lis, J.T., 2010. Chromatin landscape dictates HSF binding to target DNA elements. *PLoS Genet.* 6, e1001114.
- Guo, X., Liang, J., Lin, R., Zhang, L., Zhang, Z., Wu, J., Wang, X., 2022. Single-cell transcriptome reveals differentiation between adaxial and abaxial mesophyll cells in *Brassica rapa*. *Plant Biotechnol. J.* 20, 2233–2235.
- Hao, Y., Hao, S., Andersen-Nissen, E., Mauck III, W.M., Zheng, S., Butler, A., Lee, M.J., Wilk, A.J., Darby, C., Zager, M., Hoffman, P., Stoeckius, M., Papalexi, E., Mimitou, E.P., Jain, J., Srivastava, A., Stuart, T., Fleming, L.M., Yeung, B., Rogers, A.J., McElrath, J.M., Blish, C.A., Gottardo, R., Smibert, P., Satija, R., 2021. Integrated analysis of multimodal single-cell data. *Cell* 184, 3573–3587.
- Hatch, M.D., Kagawa, T., 1974. NAD malic enzyme in leaves with C4-pathway photosynthesis and its role in C4 acid decarboxylation. *Arch. Biochem. Biophys.* 160, 346–349.
- Hibberd, J.M., Covshoff, S., 2010. The regulation of gene expression required for C4 photosynthesis. *Annu. Rev. Plant Biol.* 61, 181–207.
- Hu, B., Jin, J., Guo, A.Y., Zhang, H., Luo, J., Gao, G., 2015. Gsds 2.0: an upgraded gene feature visualization server. *Bioinformatics* 31, 1296–1297.
- Islam, M.T., Liu, Y., Hassan, M.M., Abraham, P.E., Merlet, J., Townsend, A., Jacobson, D., Buell, C.R., Tuskan, G.A., Yang, X., 2024. Advances in the application of single-cell transcriptomics in plant systems and synthetic biology. *Biodata Res* 6, 29.
- Jacob, P., Hirt, H., Bendahmane, A., 2017. The heat-shock protein/chaperone network and multiple stress resistance. *Plant Biotechnol. J.* 15, 405–414.
- Khan, J.A., Wang, Q., Sjölund, R.D., Schulz, A., Thompson, G.A., 2007. An early nodulin-like protein accumulates in the sieve element plasma membrane of *Arabidopsis*. *Plant Physiol.* 143, 1576–1589.
- Khoshravesh, R., Hoffmann, N., Hanson, D.T., 2022. Leaf microscopy applications in photosynthesis research: identifying the gaps. *J. Exp. Bot.* 73, 1868–1893.
- Kim, D., Paggi, J.M., Park, C., Bennett, C., Salzberg, S.L., 2019. Graph-based genome alignment and genotyping with HISAT2 and HISAT-genotype. *Nat. Biotechnol.* 37, 907–915.
- Kim, J.Y., Symeonidis, E., Pang, T.Y., Denyer, T., Weidauer, D., Bezrutczyk, M., Miras, M., Zöllner, N., Hartwig, T., Wudick, M.M., Lercher, M., Chen, L.Q., Timmermans, M.C.P., Frommer, W.B., 2021. Distinct identities of leaf phloem cells revealed by single cell transcriptomics. *Plant Cell* 33, 511–530.
- Li, P., Ponnala, L., Gandomi, N., Wang, L., Si, Y., Tausta, S.L., Kebrom, T.H., Provart, N., Patel, R., Myers, C.R., Reidel, E.J., Turgeon, R., Liu, P., Sun, Q., Nelson, T., Brutnell, T.P., 2010. The developmental dynamics of the maize leaf transcriptome. *Nat. Genet.* 42, 1060–1067.
- Liu, H., Hu, D., Du, P., Wang, L., Liang, X., Li, H., Lu, Q., Li, S., Liu, H., Chen, X., Varshney, R.K., Hong, Y., 2021. Single-cell RNA-seq describes the transcriptome landscape and identifies critical transcription factors in the leaf blade of the allotetraploid peanut (*Arachis hypogaea* L.). *Plant Biotechnol. J.* 19, 2261–2276.
- Liu, Z., Zhou, Y., Guo, J., Li, J., Tian, Z., Zhu, Z., Wang, J., Wu, R., Zhang, B., Hu, Y., Sun, Y., Shangguan, Y., Li, W., Li, T., Hu, Y., Guo, C., Rochaix, J.D., Miao, Y., Sun, X., 2020. Global dynamic molecular profiling of stomatal lineage cell development by single-cell RNA sequencing. *Mol. Plant* 13, 1178–1193.
- Liu, Z., Yu, X., Qin, A., Zhao, Z., Liu, Y., Sun, S., Liu, H., Guo, C., Wu, R., Yang, J., Hu, M., Bawa, G., Sun, X., 2022. Research strategies for single-cell transcriptome analysis in plant leaves. *Plant J.* 112, 27–37.
- Livak, K.J., Schmittgen, T.D., 2001. Analysis of relative gene expression data using real-time quantitative PCR and the 2^{-ΔΔCt} method. *Methods* 25, 402–408.
- Lopez-Anido, C.B., Vatén, A., Smoot, N.K., Sharma, N., Guo, V., Gong, Y., Anleu Gil, M.X., Weimer, A.K., Bergmann, D.C., 2021. Single-cell resolution of lineage trajectories in the *Arabidopsis* stomatal lineage and developing leaf. *Dev. Cell* 56, 1043–1055.
- Ludwig, M., 2016. The roles of organic acids in C4 photosynthesis. *Front. Plant Sci.* 7, 647.
- Majeran, W., Cai, Y., Sun, Q., van Wijk, K.J., 2005. Functional differentiation of bundle sheath and mesophyll maize chloroplasts determined by comparative proteomics. *Plant Cell* 17, 3111–3140.
- Majeran, W., van Wijk, K.J., 2009. Cell-type-specific differentiation of chloroplasts in C4 plants. *Trends Plant Sci.* 14, 100–109.
- Martinère, A., Fiche, J.B., Smokvarska, M., Mari, S., Alcon, C., Dumont, X., Hematy, K., Jaillais, Y., Nöllmann, M., Maurel, C., 2019. Osmotic stress activates two reactive oxygen species pathways with distinct effects on protein nanodomains and diffusion. *Plant Physiol.* 179, 1581–1593.
- Miyake, H., Maeda, E., 1978. Starch accumulation in bundle sheath chloroplasts during the leaf development of C3 and C4 plants of the Gramineae. *Can. J. Bot.* 56, 880–882.
- Morabito, S., Miyoshi, E., Michael, N., Shahin, S., Martini, A.C., Head, E., Silva, J., Leavy, K., Perez-Rosendahl, M., Swarup, V., 2021. Single-nucleus chromatin accessibility and transcriptomic characterization of Alzheimer's disease. *Nat. Genet.* 53, 1143–1155.
- Procko, C., Lee, T., Borsuk, A., Bargmann, B.O.R., Dabi, T., Nery, J.R., Estelle, M., Baird, L., O'Connor, C., Brodersen, C., Ecker, J.R., Chory, J., 2022. Leaf cell-specific and single-cell transcriptional profiling reveals a role for the palisade layer in UV light protection. *Plant Cell* 34, 3261–3279.
- Reyt, G., Chao, Z., Flis, P., Salas-González, I., Castrillo, G., Chao, D.Y., Salt, D.E., 2020. Uclacyanin proteins are required for lignified nanodomain formation within casparyan strips. *Curr. Biol.* 30, 4103–4111.
- Rombauts, S., Déhais, P., Van Montagu, M., Rouzé, P., 1999. PlantCARE, a plant cis-acting regulatory element database. *Nucleic Acids Res.* 27, 295–296.
- Sage, R.F., 2017. A portrait of the C4 photosynthetic family on the 50th anniversary of its discovery: species number, evolutionary lineages, and Hall of Fame. *J. Exp. Bot.* 68, 4039–4056.
- Shannon, P., Markiel, A., Ozier, O., Baliga, N.S., Wang, J.T., Ramage, D., Amin, N., Schwikowski, B., Ideker, T., 2003. Cytoscape: a software environment for integrated models of biomolecular interaction networks. *Genome Res.* 13, 2498–2504.
- Slewinski, T.L., 2011. Diverse functional roles of monosaccharide transporters and their homologs in vascular plants: a physiological perspective. *Mol. Plant* 4, 641–662.
- Sonawane, B.V., Sharwood, R.E., Whitney, S., Ghannoum, O., 2018. Shade compromises the photosynthetic efficiency of NADP-ME less than that of PEP-CK and NAD-ME C4 grasses. *J. Exp. Bot.* 69, 3053–3068.
- Suzuki, R., Shimodaira, H., 2006. Pvclust: an R package for assessing the uncertainty in hierarchical clustering. *Bioinformatics* 22, 1540–1542.
- Tao, S., Liu, P., Shi, Y., Feng, Y., Gao, J., Chen, L., Zhang, A., Cheng, X., Wei, H., Zhang, T., Zhang, W., 2022. Single-cell transcriptome and network analyses unveil key transcription factors regulating mesophyll cell development in maize. *Genes* 13, 374.
- Tenorio Berrio, R., Verstaen, K., Vandamme, N., Pevernagie, J., Achon, I., Van Duyse, J., Van Isterdael, G., Saeyns, Y., De Veylder, L., Inzé, D., Dubois, M., 2022. Single-cell transcriptomics sheds light on the identity and metabolism of developing leaf cells. *Plant Physiol.* 188, 898–918.
- Wang, Q., Wu, Y., Peng, A., Cui, J., Zhao, M., Pan, Y., Zhang, M., Tian, K., Schwab, W., Song, C., 2022. Single-cell transcriptome atlas reveals developmental trajectories and a novel metabolic pathway of catechin esters in tea leaves. *Plant Biotechnol. J.* 20, 2089–2106.
- Wang, W., Chen, D., Liu, D., Cheng, Y., Zhang, X., Song, L., Hu, M., Dong, J., Shen, F., 2020. Comprehensive analysis of the *Gossypium hirsutum* L. respiratory burst oxidase homolog (*Ghrobh*) gene family. *BMC Genom.* 21, 91.
- Wang, Y., Huan, Q., Li, K., Qian, W., 2021. Single-cell transcriptome atlas of the leaf and root of rice seedlings. *J. Genet. Genomics* 48, 881–898.
- Wu, T., Hu, E., Xu, S., Chen, M., Guo, P., Dai, Z., Feng, T., Zhou, L., Tang, W., Zhan, L., Fu, X., Liu, S., Bo, X., Yu, G., 2021. ClusterProfiler 4.0: a universal enrichment tool for interpreting omics data. *Innovation* 2, 100141.
- Xie, Y., Jiang, S., Li, L., Yu, X., Wang, Y., Luo, C., Cai, Q., He, W., Xie, H., Zheng, Y., Xie, H., Zhang, J., 2020. Single-cell RNA sequencing efficiently predicts transcription factor targets in plants. *Front. Plant Sci.* 11, 603302.
- Xu, X., Liu, W., Liu, X., Cao, Y., Li, X., Wang, G., Fu, C., Fu, J., 2022. Genetic manipulation of bermudagrass photosynthetic biosynthesis using *Agrobacterium*-mediated transformation. *Physiol. Plantarum* 174, e13710.
- Yer, E.N., Baloglu, M.C., Ayan, S., 2018. Identification and expression profiling of all Hsp family member genes under salinity stress in different poplar clones. *Gene* 678, 324–336.
- Zhang, B., Chen, S., Liu, J., Yan, Y.B., Chen, J., Li, D., Liu, J.Y., 2022. A high-quality haplotype-resolved genome of common bermudagrass (*Cynodon dactylon* L.) provides insights into polyploid genome stability and prostrate growth. *Front. Plant Sci.* 13, 890980.
- Zhang, B., Liu, J., Wang, X., Wei, Z., 2018. Full-length RNA sequencing reveals unique transcriptome composition in bermudagrass. *Plant Physiol. Biochem.* 132, 95–103.